Organic Electronics 13 (2012) 645–651

Contents lists available at SciVerse ScienceDirect

Organic Electronics

journal homepage: www.elsevier.com/locate/orgel

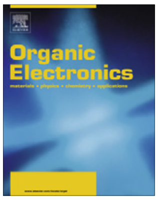

Significance of irreversible formation of “electromer” in 1-bis[4-[N,N-di(4-tolyl)amino]phenyl]-cyclohexane layer associated with the stability of deep blue phosphorescent organic light emitting diodes

Soonnam Kwon, Kyung-Ryang Wee, Chyongjin Pac *, Sang Ook Kang *

Department of Advanced Materials Chemistry, Korea University, Sejong, Chungnam 339-700, South Korea

ARTICLE INFO

Article history:
Received 7 October 2011
Received in revised form 30 December 2011
Accepted 31 December 2011
Available online 16 January 2012

Keywords:
Electromer
Defect sites
Stability
Deep blue PHOLED

ABSTRACT

We demonstrate that injection of electrons in 1-bis[4-[N,N-di(4-tolyl)amino]phenyl]-cyclohexane (TAPC) layer irreversibly induces defect sites responsible for “electromer” emission. We also show that the defects alter the charge transporting properties of TAPC layer to influence the charge balance of iridium(III)[bis(4,6-difluorophenyl)pyridinato-N,C$^{2'}$]tetrakis(1-pyrazolyl)borate (FIr6) based deep blue phosphorescent organic light emitting diodes (PHOLED). The present investigation implies that deep-blue PHOLEDs should be carefully designed for the emission zone to be located far enough from the TAPC layer so as to avoid or minimize the emission from TAPC layer.

1. Introduction

1-Bis[4-[N,N-di(4-tolyl)amino]phenyl]-cyclohexane (TAPC) was first used as a material for hole-transporting layer (HTL) in historical Ching Tang’s first report on two layer organic light emitting diode (OLED) [1]. Recently, owing to its unique characteristics, such as high triplet energy (T1 = 2.87 eV) [2], high hole mobility [3], high lowest unoccupied molecular orbital (LUMO) level (2.0 eV) [4,5], and adequate highest occupied molecular orbital (HOMO) level (5.5 eV), it is widely used in deep blue phosphorescent OLED (PHOLED) as a triplet exciton and electron blocking layer, resulting in high performance [4–10]. However, there still remains the problem of stability of deep blue PHOLED. It is well known that, blue PHOLEDs suffer from serious stability issue [11,12]. This may due to the instability of blue emitters itself or thermal and electrochemical instability of host, HTL, and electron transporting layer (ETL) materials. TAPC has been expected to be one of the causes of instability of the blue device due to its low T_g [13,14].

However, several recent reports on the deep blue PHOLED devices and materials suggest that more critical issue other than thermal property may cause fast decay of deep blue PHOLED using TAPC. In our previous report, irreversible changes of color coordinates were observed as the current density is increased, which is an indication of irreversible change of device characteristics [8]. Fukagawa et al. reported that electromer emission can be observed if the recombination zone is formed near TAPC/EML, resulting in low current efficiency of the device [10]. Such irreversible change might arise from formation of various defect sites during operation of devices. For unperturbed solid, electrons can transport between LUMO levels of adjacent molecules [16]. However, if defect sites exist, electron localization on the defect site impedes electron transport and increases the probability for the excess electron to recombine directly with a HOMO located hole on the other molecule [16]. Concerning defect-site formation in TAPC thin film, and interesting observation was first reported by Kalinowski et al. [15,16]; peculiar emission called

---

* Corresponding authors.
E-mail addresses: jjpac@korea.ac.kr (C. Pac), sangok@korea.ac.kr (S.O. Kang).

1566-1199/$ - see front matter © 2012 Elsevier B.V. All rights reserved.
doi:10.1016/j.orgel.2011.12.022

"electromer" emission different from any other photoluminescences appears upon injecting electrons and holes into a TAPC film, being attributed to unique defect sites existing in the TAPC film. Since this publication by Kalinowski, unique emissions from light emitting diodes have been often ascribed as electromer emissions without detailed analysis. Although electromer sites can be considered to be related with performances and stability of devices, however, little has been investigated on what is the origin of the electromer-site formation and on how the defect sites would affect device characteristics. In the present investigation, careful measurements were performed on time dependence of electroluminescence (EL) for devices using a TAPC film. On the basis of observations, we demonstrate that the defect sites responsible for the electromer emission are created by the injection of electrons into the TAPC film. And we also show that any unexpected electron current which are injected into TAPC film can cause such defects, resulting in irreversible change in charge transporting properties of the TAPC film. The effect of such defect sites on the early stability of iridium(III)[bis(4,6-difluorophenyl)pyridinato-N,C$^{2'}$]tetrakis(1-pyrazolyl)borate (FIr6) based deep blue PHOLED is also investigated.

2. Experiment

Bis(4-(4,5-Diphenyl-4H-1,2,4-triazol-3-yl)phenyl)dimethylsilane (SiTAZ) were prepared using the methods reported in the literature [8]. Commercially available materials, FIr6, TAPC, and *N*,*N*8-dicarbazolyl-3,5-benzene (mCP), were used as received. The absorption and photoluminescence (PL) spectra were recorded on a Shimadzu UV-3101PC UV/Vis/NIR spectrometer and a Varian Cary Eclipse fluorescence spectrometer, respectively. The current–voltage characteristics of OLEDs were measured using Keithley 236. The EL spectra, luminance, and the CIE color coordinates were measured using a spectroradiometer (Photo Research PR650). For the transient EL measurements, a source measure unit (Keithley 2400) was used as an constant current source and the EL light was passed through optical filters, to which a photomultiplier tube (PMT, Oriel 77346) was attached. A preamplifier (Stanford Research System SR240A) was used prior to the final data acquisition.

The OLED devices were fabricated on glass substrates precoated with a 150 nm ITO layer with a sheet resistance of 10 Ω/square. The ITO glass was precleaned using a conventional solvent cleaning method. The ITO surface was cleaned again with a UV ozone treatment immediately before depositing the HTL. The organic, LiF, and Al layers were deposited sequentially onto the substrate without breaking the vacuum.

3. Results and discussion

3.1. Relationship between electron injection and electromer emission in TAPC film

Fig. 1(a) illustrates PL spectra of TAPC solution and film, and compares them to EL spectrum of device I shown in Fig. 2. In contrast to the solution spectrum, as-deposited film shows an additional weak emission at longer wavelength, which can be assigned as excimer emission. Upon heating the film at 100 °C, the excimer emission grew remarkably. This behavior can be easily understood, because the thermal treatment should cause crystallization in the film to enhance molecular stacking favorable for excimer formation.

To examine the electromer emission of TAPC, the device with the structure of ITO(150 nm)/TAPC(200 nm)/LiF (0.5 nm)/Al(60 nm), was fabricated. However, only hole current was detected without any emission of light. This may be due to high energy barrier (~2.1 eV) for electron injection from cathode to LUMO of TAPC compared to hole injection barrier of ~0.7 eV. To efficiently inject electrons into TAPC, SiTAZ layer with high LUMO level of 2.5 eV is inserted between TAPC and cathode with the device structure of ITO(150 nm)/NPB(30 nm)/TAPC(15 nm)/SiTAZ(60 nm)/LiF(0.5 nm)/Al(60 nm) (device I). Exciton is expected to be formed inside the TAPC layer because of deep HOMO level of SiTAZ. If electric field is increased over a threshold value, electron would be injected into TAPC, producing light emission as a result of radiative recombination of excitons. As shown in Fig. 1(a), the EL of device I reveals unique spectral features entirely different from PL emitted from either solution or solids before and after thermal annealing. Two comparable features are seen: one has peak around 430 nm, and the other around 580 nm. The feature around 580 nm can be definitely assigned as electromer of TAPC layer [15]. In case of the feature around 430 nm (feature A), two decay pathways of exciton are possible. One is excimer formed in TAPC layer (around 435 nm), and the other is exciplex [22] formed at the interface of TAPC and SiTAZ layers (around 420 nm). Even though the excimer peak of heated film and the feature A of EL spectrum look very similar to each other, we cannot assign it definitely as excimer emission exclusively, considering the following observations. First, the main peak position of feature A changes as a function of time or as the driving condition changes, as can be seen in Figs. 2(a) and 3(b). Second, the feature A in Fig. 2(a) consists of at least two sub-peaks, of which relative intensities change as a function of time. Furthermore, the feature A cannot be assigned as a first singlet excited state of NPB from the possible injection of electrons into NPB layer, because the device without NPB layer showed the same feature.

Fig. 2(a) illustrates the dynamic change of EL spectra as a function of time at constant current driving condition (0.125 mA/cm^2). Due to the finite data acquisition time of the spectrometer (PR650) at the low level of luminance (around 1.5 cd/m^2), the data were taken every 15 s. At first, the intensity of electromer feature is lower than that of feature A, and after 75 s, the intensity of the former becomes larger than that of the later. If we could measure spectra faster, the initial intensity of the electromer peak is expected to be zero. To observe the initial growing of the electromer peak, EL emission was optically filtered by a high pass filter (500 nm), optically focused, and amplified by a PMT as shown in inset of Fig. 2(b). The photocurrent signal grows up continuously from background level and is saturated to a certain level after about 75 s from turn on of constant current (0.125 mA/cm^2). One more thing to

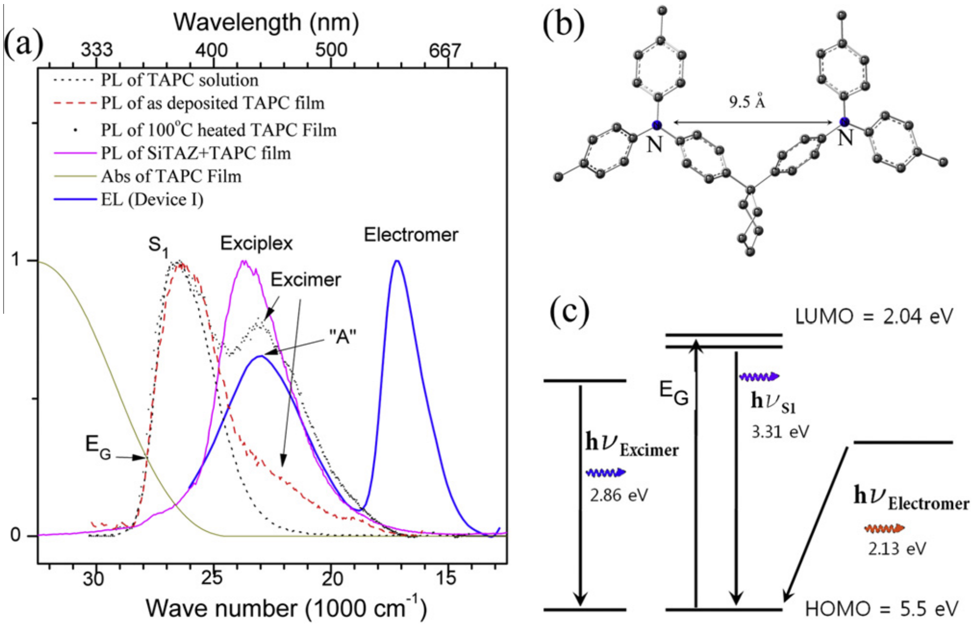

Fig. 1. (a) Absorption and PL spectra of 100 nm thick as-deposited and heated TAPC film vacuum deposited onto fussed silica substrate. The PL spectra are compared with PL of dilute solution of TAPC (Dichloromethane, 10 μmol). PL of mixed film of TAPC and SiTAZ, and EL of device I are also shown. (b) Optimized geometry of neutral ground state molecule of TAPC, calculated by B3LYP/6-31G(D,P) level of theory on the platform of Gaussian 09 [17]. (c) Energy level diagrams of each emission found from PL and EL of TAPC film in (a).

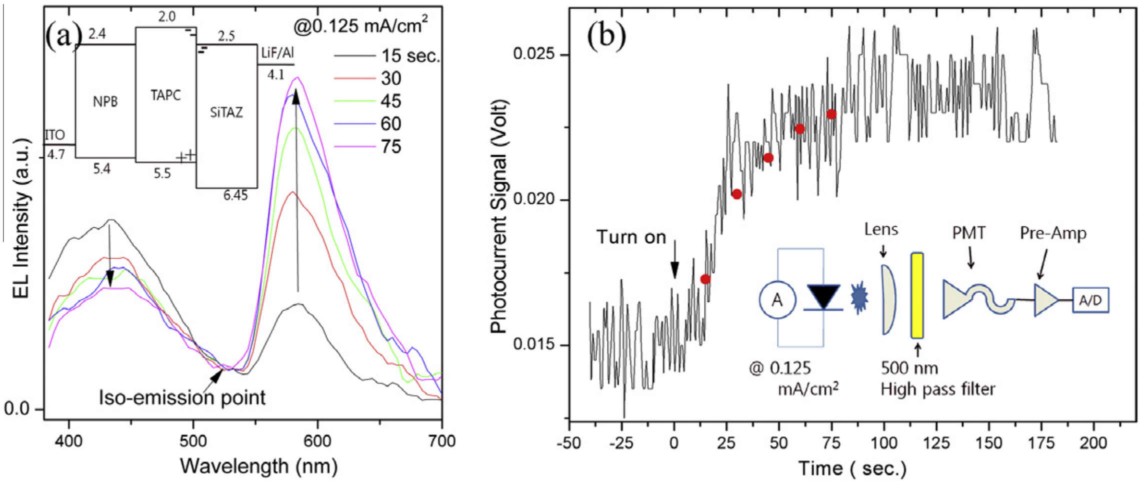

Fig. 2. (a) Change of EL spectra as a function of time, in which the device is driven at constant current of 0.125 mA/cm^2. Inset: energy level diagram of device I. (b) Time evolution of integrated intensity of electromer spectrum (plain line), and comparison with the peak intensity data obtained from (a) (red filled circles). Inset: schematic diagram of experimental apparatus for obtaining the integrated intensity of electromer spectrum. (For interpretation of the references to color in this figure legend, the reader is referred to the web version of this article.)

be taken attention is the existence of iso-emission point [19–21] around 530 nm, as can be seen in Fig. 2(a). The EL spectra shorter than this point decrease as a function of time, and vice versa for those larger than the point. The results of Fig. 2 mean that the current flow results in the initial formation of feature A followed by apparent conversion of feature A site to electromer site or by increasing formation of electromer site accompanied by energy transfer from feature A site. The appearance of iso-emissive point suggests the apparent stoichiometric relationship between the feature A and electromer emission.

3.2. Evidence of irreversible formation of electromer in TAPC film

The above process seems irreversible. To prove this, the characteristics of two comparative devices with the structure of ITO/NPB(30 nm)/TAPC(15 nm)/SiTAZ(60 nm)/

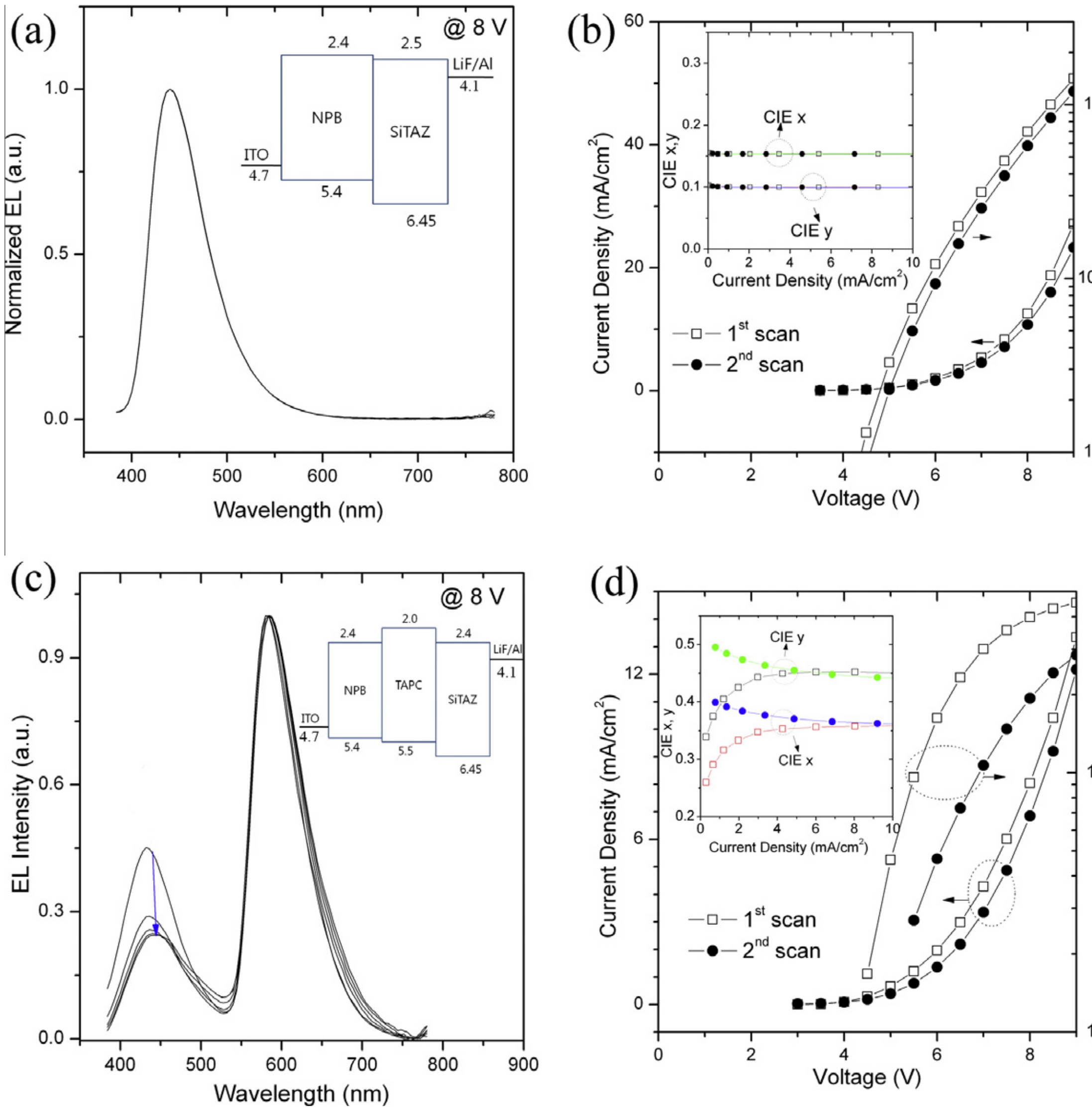

Fig. 3. (a) Normalized EL spectra taken 6 times in 90 s driven at constant voltage of 8 V of the device II: ITO(150 nm)/NPB (45 nm)/SiTAZ(60 nm)/LiF(0.5 nm)/Al(60 nm). (b) Current density–voltage and luminance–voltage curves of device II, in which the measurements were repeated twice. Inset: CIE *x* and *y* coordinates-current density curves. (c) The same measurements as those of (a), in which the device I was used with the structure of ITO(150 nm)/NPB(30 nm)/TAPC(15 nm)/SiTAZ(60 nm)/ LiF(0.5 nm)/Al(60 nm). (d) Device characteristics of the deivice I, and the same measurements were made as those of (b). Inset: CIE *x* and *y*-current density curves of device II, in which successive two measurements are plotted together.

LiF(0.5 nm)/Al(60 nm) (device I) and ITO/NPB(45 m)/SiTAZ(60 nm)/LiF(0.5 nm)/Al(60 nm) (device II) were investigated as shown in Fig. 3. In the case of device II, only the singlet exciton peak of NPB is found in the EL spectra, and the spectra do not show any dependence on time, which is contrary to the result of device I in Fig. 3(c). The irreversible character of the formation of electromer is more remarkably observed if we examine the current density–voltage, luminance-voltage, and color coordinates-current density curves, as comparatively shown in Fig. 3(b) and (d). In case of device II, the device characteristics do not change significantly after repeated measurements. Whereas, device I show dramatic change in luminance and color coordinates when the device is measured for the second time. We tried to recover the device with various methods, including reverse biasing. However, the change of the device characteristics is irreversible. The cause of the change in luminance and color coordinates is the reduction of feature A and the increase of electromer peak. And it seems that the electromer emission is not efficient process, because the luminance efficiency decreases as the electromer emission increases.

The above observations support the supposition that the defect sites are developed by electrons injected into TAPC layer: Initially only the excitations of feature A exist, defect sites are induced near the sites of feature A, and the defect sites increase as a function of time.

However, there still remains a question about the process, by which the defect sites are developed. Even though further study concerning the mechanisms is needed, we can suppose the following mechanisms. One is the possible local morphological change induced by local coulomb interaction between hole and electron. Otherwise, unstable anion state of TAPC may have formed into unexpected defect products, which is analogous to the degradation mechanism of Alq3 [23]. We tried to measure any additional absorption spectrum after the formation of electromer. However, to our limit of measurement sensitivity, no sign of new chemical was found.

3.3. Influence of electromer formation on the device stability of deep blue PHOLED

From the above discussion, it is likely that electron injection into TAPC layer may induce irreversible change of the TAPC film, resulting in changes in the whole device characteristics. To examine this, two different devices were fabricated. One (device III) is designed to have low current efficiency on purposely to allow parts of electrons to pass through EML without recombination with holes. And the other (device IV) is a normal device with high efficiency.

The device structure of device III is ITO(150 nm)/NPB(30 nm)/TAPC(15 nm)/mCP(20 nm)/mCP:FIr6 (2 wt.%) (5 nm)/SiTAZ(40 nm)/LiF(0.5 nm)/Al(60 nm), in which the thickness of FIr6 doped region is narrow, and the doping concentration is low compared to the conventional devices [7]. The device characteristics were measured for two different devices with the same device structure, one is virgin device and the other is the device experienced 1 h of aging at constant current of 1.0 mA/cm^2, as shown in Fig. 4(a). The maximum current efficiency of the initial device was degraded from 9.0 cd/A (EQE of 5.5%) to 2.7 cd/A (EQE of 1.46%) for aged device, and the turn on voltage was delayed from 4.5 to 6.0 V. Inset of Fig. 4(b) illustrates that the driving voltage at constant current of 1.0 mA/cm^2 grows up fast from 6.0 to 7.55 V, and the main peak intensity decays fast as a function of time. Fig. 4(b) shows the change of normalized EL spectra as a function of time. At first, only the mCP host [18] and FIr6 emission can be observed without electromer emission. The appearance of mCP emission is caused by inefficient energy transfer from host to dopant due to low concentration of FIr6 and also by the emission from un-doped mCP layer, which indicate the electron penetration into the un-doped region. As time goes on, electromer peak and feature A grow up. These indicate that the emission zone has enlarged to TAPC/mCP interface as time elapses at constant current driving. Because the amount of electrons injected into TAPC per unit time is much lower than that of device I, the rate of development of electromer peak is relatively low compared to that of device I of Fig. 2.

Fig. 5 illustrates the characteristics of the device IV with high current efficiency (maximum efficiency of 24 cd/A) for comparative study to the results of device III. The device structure is ITO(150 nm)/NPB(30 nm)/TAPC(15 nm)/mCP (5 nm)/mCP:FIr6 (10 wt.%) (20 nm)/SiTAZ(40 nm)/LiF(0.5 nm)/Al(60 nm). Turn on voltage was delayed from 4.5 to 5.0 V, and driving voltage was increased by 0.5 V after 1 h aging of the device at constant current of 1.0 mA/cm^2, as shown in Fig. 5(a). The voltage shifts are remarkably reduced compared to those of device III. The main peak intensity maintained up to 0.64 of its initial value, which is relatively high value compared to that of device III (0.23) of Fig. 4. Contrary to the result of device III, normalized EL spectra do not show any remarkable change after the same aging. However, the enlarged views of EL spectra show slight indication of growing of the electromer peak. This indicates that even the high efficiency device allows small amount of electrons to pass through into the TAPC layer.

Comparing the device results of Fig. 4 to those of Fig. 5, we can deduce the following two observations. First, the increase of electromer peak is dependent on time. Therefore, considering the results of Fig. 1(b), together with the constant current driving condition, the electromer peak height can be related to the amount of injected electrons

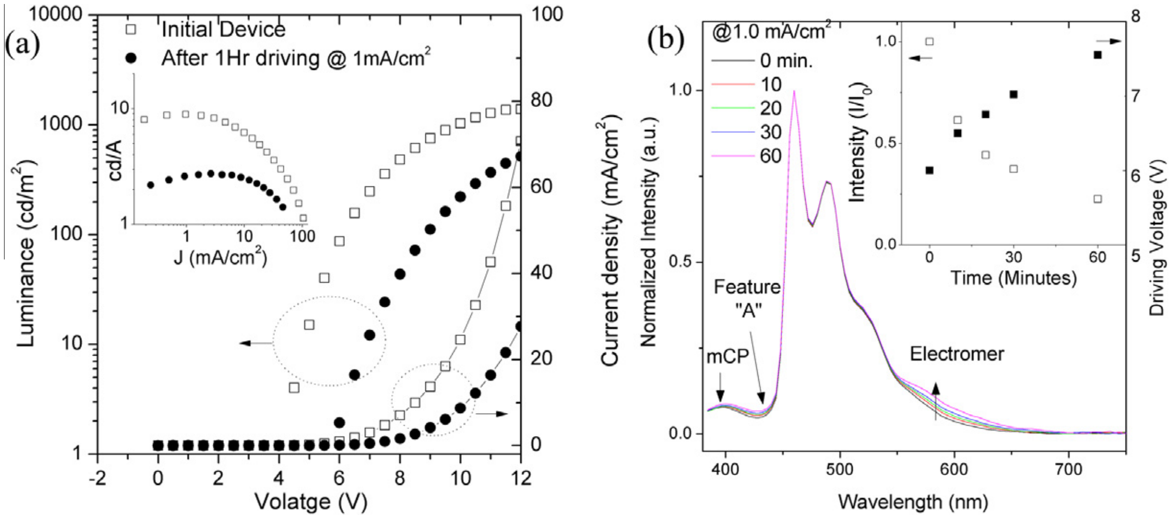

Fig. 4. Low efficiency device (device III) with the structure of ITO(150 nm)/NPB(30 nm)/TAPC(15 nm)/mCP(20 nm)/mCP:FIr6 2 wt.% (5 nm)/SiTAZ(40 nm)/LiF(0.5 nm)/Al(60 nm). (a) Device characteristics measured for the first time (hollow squares), and after 1 h aging (filled circles). (b) Change of normalized EL spectra as a function of time. Inset: Change of intensity and driving voltage as a function of time.

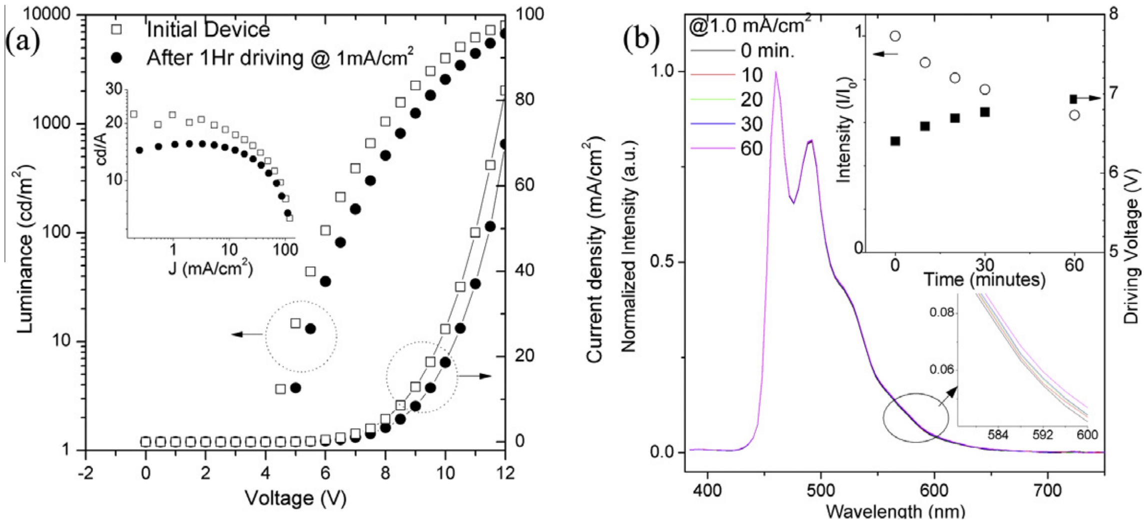

Fig. 5. High efficiency device (device IV) with the structure of ITO(150 nm)/NPB(30 nm)/TAPC(15 nm)/mCP(5 nm)/mCP:FIr6 10 wt.% (20 nm)/SiTAZ(40 nm)/LiF(0.5 nm)/Al(60 nm). (a) Device characteristics measured for the first time (hollow squares), and after 1 h aging (filled circles). (b) Change of normalized EL spectra as a function of time. Inset: Change of intensity and driving voltage as a function of time.

Table 1
Comparison of device characteristics before and after aging.

	Initial device			Aged device[a]		
	Von (V)	Max. C. E. (cd/A)	J^b @ 10 V (mA/cm^2)	Von (V)	Max C. E. (cd/A)	J @ 10 V (mA/cm^2)
Device III	4.5	8.9	24.6	6	2.74	8.7
Device IV	4.5	23.8	26.4	5	16.6	18.6

[a] Device which have biased at constant current of 1 mA/cm^2 for 1 h.
[b] Current density.

into TAPC layer. Second, the rate of increase of driving voltage of device III is abnormally high compared to that of device IV, even though the same materials were used and most of the interfaces are similar for both of the devices. Differences in doping ratios and thicknesses of doped region do not influence on the driving voltage, which is evident from similar voltage-current characteristics for both of the devices for initial devices (Table 1). However, after aging, only the device III showed abrupt decrease in current. Therefore, the origin of fast rise of driving voltage can be ascribed to the change of electronic properties of TAPC layer or interface between TAPC and mCP, which is induced by the electron current reaching to the TAPC layer. It is expected that the majority of current passing through the interface of TAPC and mCP is hole. This also implies that the increase of defect sites impedes not only electron transport but also hole transport near the interface of TAPC and EML, finally altering the charge transporting properties of the whole device.

4. Conclusion

In conclusion, electron current injected into TAPC layer make defect sites. Electrons are trapped in these sites and form electromer. The formation of the defect sites increase as a function of time and after some time, electromer emission prevails. This process is irreversible. The defect sites can be interpreted as morphological change of the TAPC film or chemical change from unstable anion state of TAPC molecule. After the formation of defect sites, the charge transporting properties of TAPC layer is altered, influencing the device characteristics. Therefore, when using TAPC as a triplet exciton blocking layer, device should be carefully designed for the emission zone to be located far enough from the TAPC layer so as to avoid or minimize emission from the TAPC layer.

Acknowledgements

This research was supported by the Basic Science Research Program through the National Research Foundation of Korea (NRF) funded by the Ministry of Education, Science, and Technology (MEST) of Korea (2011-0018595) and by the Center for Next Generation Dye-Sensitized Solar Cells (No. 2011-0001055). We also acknowledge the Industrial strategic technology development program (10030814, Development of Organic materials for OLED) funded by the Ministry of Knowledge Economy (MKE, Korea).

References

[1] C.W. Tang, S.A. VanSlyke, Appl. Phys. Lett. 51 (1987) 913.
[2] K. Goushi, R. Kwong, J.J. Brown, H. Sasabe, C. Adachi, J. Appl. Phys. 95 (2004) 7798.

[3] H. Sasabe, E. Gonmori, T. Chiba, Y.-J. Li, D. Tanaka, S.-J. Su, T. Takeda, Y.-J. Pu, K. Nakayama, J. Kido, Chem. Mater. 20 (2008) 5951.

[4] Y. Zheng, S.-H. Eom, N. Chopra, J. Lee, F. So, J. Xue, Appl. Phys. Lett. 92 (2008) 223301.

[5] S.-H. Eom, Y. Zheng, E. Wrzesniewski, J. Lee, N. Chopra, F. So, J. Xue, Org. Electron. 10 (2009) 686.

[6] J. Lee, J.-I. Lee, J.-W. Lee, H.Y. Chu, Org. Electron. 11 (2010) 1159.

[7] S. Kwon, K.-R. Wee, J.W. Kim, S.O. Kang, Appl. Phys. Lett. 97 (2010) 023309.

[8] S. Kwon, K.-R. Wee, A.-L. Kim, S.O. Kang, J. Phys. Chem. Lett. 1 (2010) 295.

[9] N. Chopra, J.S. Swensen, E. Polikarpov, L. Cosimbescu, F. So, A.B. Padmaperuma, Appl. Phys. Lett. 97 (2010) 033304.

[10] H. Fukagawa, S. Irisa, H. Hanashima, T. Shimizu, S. Tokito, N. Yokoyama, H. Fujikake, Org. Electron. 12 (2011) 1638.

[11] M.-H. Tsai, Y.-H. Hong, C.-H. Chang, H.-C. Su, C.-C. Wu, A. Matoliukstyte, J. Simokaitiene, S. Grigalevicius, J.V. Grazulevicius, C.-P. Hsu, Adv. Mater. 19 (2007) 862.

[12] S.-J. Su, E. Gonmori, H. Sasabe, J. Kido, Adv. Mater. 20 (2008) 4189.

[13] P. Strohrigl, J.V. Grazulevicius, Adv. Mater. 14 (2002) 1439.

[14] W.-Y. Hung, L.-C. Chi, W.-J. Chen, Y.-M. Chen, S.-H. Chou, K.-T. Wong, J. Mater. Chem. 20 (2010) 10113.

[15] J. Kalinowski, G. Giro, M. Cocchi, V. Fattori, P. Di Marco, Appl. Phys. Lett. 76 (2000) 2352.

[16] J. Kalinowski, Organic Light-Emitting Diodes Priciples Characteristics and Precesses, Marcel Dekker, New York, 2005 (Chapter 2).

[17] Gaussian 09 (Revision A.02), Gaussian Inc., Wallingford, CT, 2009.

[18] T. Tsuboi, H. Murayama, S.-J. Yeh, M.-F. Wu, C.-T. Chen, Opt. Mater. 31 (2008) 366.

[19] B. Stevens, M.I. Ban, Trans. Faraday Soc. 60 (1964) 1515.

[20] A.J.H. Al-Wattar, M.D. Lumb, Chem. Phys. Lett. 8 (1971) 331.

[21] H. Lin, Y. Weng, H. Huang, Q. He, M. Zheng, F. Bai, Appl. Phys. Lett. 84 (2004) 2980.

[22] G. Li, C.H. Kim, Z. Zhou, J. Shinar, K. Okumoto, Y. Shirota, Appl. Phys. Lett. 88 (2006) 253505.

[23] H. Aziz, Z.D. Popovic, N.-X. Hu, A.-H. Hor, G. Xu, Science 283 (1999) 1900.